Food Chemistry 448 (2024) 139060

Contents lists available at ScienceDirect

Food Chemistry

journal homepage: www.elsevier.com/locate/foodchem

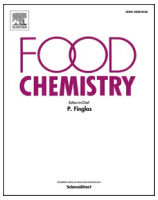

Microwave-assisted esterification and electro-enhanced solid-phase microextraction of omega-3 polyunsaturated fatty acids in eggs

Xian-Chun Gu [a], Qiu-Fang Zhang [c], Yue-Hong Pang [a,b], Xiao-Fang Shen [a,b,*]

[a] State Key Laboratory of Food Science and Resources, School of Food Science and Technology, Collaborative Innovation Center of Food Safety and Quality Control in Jiangsu Province, Jiangnan University, Wuxi 214122, China
[b] International Joint Laboratory on Food Safety, Jiangnan University, Wuxi 214122, China
[c] Zibo Institute of Inspection, Testing and Metrology, Zibo 255199, Shandong, China

ARTICLE INFO

Keywords:
Omega-3 polyunsaturated fatty acids
Microwave-assisted esterification
Electro-enhanced solid-phase microextraction
Gas chromatography
Eggs

ABSTRACT

Omega-3 polyunsaturated fatty acids (ω-3 PUFAs), a type of fatty acid that has many health benefits, are of increasing concern. Herein, we developed a method for the rapid esterification and enrichment of ω-3 PUFAs in eggs, which includes microwave-assisted esterification (MAE) and electrically enhanced solid-phase microextraction (EE-SPME). Combined with gas chromatographic, efficient detection of ω-3 PUFAs was achieved in eggs. Under microwave radiation, the esterification efficiency exhibited a significant increase ranging from 5.06 to 10.65 times. The EE-SPME method reduced extraction time from 50 to 15 min. In addition, improvements in extractive fiber coating materials were explored, which ensured efficient extraction of ω-3 PUFAs. Under the optimal conditions, the method displayed a low detection limit (1.01–1.54 μg L^{-1}), good recoveries (85.82%–106.01%), and wide linear range (7.5–1000 μg L^{-1}), which was successfully applied to determine ω-3 PUFAs in real egg samples.

1. Introduction

Omega-3 polyunsaturated fatty acids (ω-3 PUFAs) are considered indispensable fatty acids, encompassing alpha-linolenic acid (ALA), eicosapentaenoic acid (EPA), and docosahexaenoic acid (DHA). These fatty acids play crucial roles in reducing blood lipids (Bakker et al., 2023), decreasing blood pressure (Bonafini, Antoniazzi, Maffeis, Minuz, & Fava, 2015), modulating cholesterol levels, preventing cardiovascular and cerebrovascular diseases (Kastelein et al., 2014), as well as fostering the growth of the brain and nervous system (Balakrishnan, Kannan, & Govindasamy, 2021). Eggs, an important part of the daily diet, are important carrier of ω-3 PUFAs, and the yolks contain high levels of phosphoproteins, which is noteworthy for the stability of ω-3 PUFAs in eggs (Marcet, Sáez-Orviz, Rendueles, & Díaz, 2022). With the development of ω-3 PUFAs egg products and the need for market management (Javed, King, Imran, Jeoh, & Naseem, 2019), the detection of ω-3 PUFAs in egg products has become increasingly important.

Gas chromatography with flame ionization detector (GC-FID) is widely used for the determination of ω-3 PUFAs in eggs (de Oliveira Mendes, Porto, Almeida, Fantini, & Sena, 2019; Grela, Knaga, Winiarska-Mieczan, & Zieba, 2020). It requires complex pre-treatment procedures including freeze-drying, saponification, esterification, extraction, and filtration (ISO17059, 2007; ISO5509, 2000). Conventional saponification esterification reactions are heated by water bath, which reaches equilibrium slowly (1−2*h*), resulting in that the PUFA is prone to be oxidized with low conversion and high energy consumption. Classical liquid-liquid extraction method requires the use of large amounts of toxic organic reagents and has significant deviation during the extraction and transfer process. In recent years, more and more studies have been focused on the optimization of fatty acid pretreatment methods.Alinafiah (Muhammad Alinafiah, Azlan, Ismail, Rashid, & N. K., 2021) used GC-FID and Weibull model for accurate quantification of fatty acid content in fish, but the implementation of these methods could not avoid the inefficiency of detection or the use of large amounts of toxic solvents (Pasupuleti, Tsai, Ponnusamy, & Chen, 2022; Sprynskyy et al., 2022).Thus, it is of great importance to develop a rapid, reliable, and efficient pre-treatment method for ω-3 PUFAs in eggs.

Microwave radiation, an innovative energy source, can be used to obtain high yields in short reaction times as well as high product purity under mild reaction conditions (Yadav, Yadav, & Ahmaruzzaman,

* Corresponding author at: State Key Laboratory of Food Science and Resources, School of Food Science and Technology, Collaborative Innovation Center of Food Safety and Quality Control in Jiangsu Province, Jiangnan University, Wuxi 214122, China.
E-mail address: xfshen@jiangnan.edu.cn (X.-F. Shen).

https://doi.org/10.1016/j.foodchem.2024.139060
Received 21 November 2023; Received in revised form 31 January 2024; Accepted 15 March 2024
Available online 21 March 2024

2023). Microwave radiation can expedite the esterification process of fatty acids, leading to rapid attainment of high yields. Duz et al. conducted a microwave-assisted alkali-catalyzed esterification process on safflower seed oil for biodiesel production, achieving a remarkable conversion rate exceeding 98.4% within a mere 6-min timeframe (Duz, Saydut, & Ozturk, 2011). Brunton et al. evaluated the fatty acid profiles of selected foods through a comparison between microwave-assisted fatty acid profiles and traditional fatty acid methyl ester. The microwave-assisted method, in contrast to traditional methods, offers simplicity, speed, and a high recovery rate (98–102%) (Brunton, Mason, & Collins, 2015). It holds significant potential as an alternative technique to conventional water bath heating, however, there were few reports about the application of microwave method to ω-3 PUFAs.

Efficient extraction of esterified ω-3 PUFAs contributes to enhance the sensitivity of the detection. Solid phase microextraction (SPME), low sample volume, solvent-free, environmentally friendly, simple and fast, is an ideal candidate for extraction of ω-3 PUFAs in eggs (Zheng, Kuang, Zhou, Gong, & Ouyang, 2023). In conventional SPME, it is a time-consuming process due to the extraction equilibrium depends mainly on free diffusion. Electro field can be used to achieve rapid extraction equilibrium by introducing an electric potential into the SPME system. Recently, our group developed the electro-enhanced solid-phase microextraction (EE-SPME) method to enrich bisphenols, which improved the extraction efficiency and shortened the extraction time (25 min to 10 min). (Y. H. Pang, Huang, Shen, & Wang, 2021; Qiao, Pang, Yan, & Shen, 2022). Therefore, our motivation was to prepare functional materials with good electrical conductivity and develop a method of EE-SPME in synergy with microwave-assisted transesterification for efficient extraction of ω-3 PUFAs.

Hydrophilic and lipophilic balanced particles (HLB) are polymers with large specific surface area, wide pH range, multifunctionality and dual lipophilicity and hydrophilicity. Herein, HLB was functionalized with aniline (An) to improve the electrical conductivity. Then HLB-An was modified onto stainless steel wires (SSW) for efficiently EE-SPME of ω-3 PUFAs, which effectively shortened the extraction time. Before extraction, the fatty acids were esterified by MAE, which improved the esterification efficiency of fatty acids. Combined with GC, sensitive detection of ω-3 PUFAs in eggs can be realized.

2. Experimental section

2.1. Reagents and materials

Anhydrous methanol, acetyl chloride, BF_3 methanol solution (14%), sulfuric acid, anhydrous potassium carbonate, all analytically pure, Sinopharm Chemical Reagent Co. Ltd.; n-hexane, chromatographically pure, Thermos Fisher Scientific (China) Co. Ltd.; Methyl Triglycerol Undecanoate (purity >99%), Methyl ALA ester, Methyl EPA ester, and Methyl DHA ester standards, Triglycerol Undecanoate (purity >99%), ALA, EPA, DHA standards were from Shanghai Amperexperiment Technology Co. SSW, two commercial SPME fibers and 5 μL micro syringe were obtained from High Pigeon (Shanghai, China). Platinum wire electrodes were purchased from Chen hua Instruments (Shanghai, China). Membranes with a pore size of 0.2 μm were obtained from Yibo Bio Ltd. Phosphate buffer solutions (PBS) were prepared by mixing 0.01 M NaH_2PO_4 and Na_2HPO_4 in different ratios, and the working solution was a mixture of fatty acid standard solution and PBS (v:v = 1:99).

2.2. Apparatus and instruments

The microwave synthesizer was a Discover single-mode focused microwave synthesis system (CEM Inc., USA). The surface morphology of synthesized nanozyme was obtained on a scanning electron microscope (SEM) (SU8100, Hitachi, Japan); The crystal structure of the synthesized material was characterized by X-ray diffraction (XRD, Bruker AXS D2 PHASER, Germany); Fourier-transform infrared (FT-IR) spectra were operated on an IS10 FT-IR spectrophotometer (Nicolet, USA); The elemental analysis of material was done via the X-ray photoelectron spectroscopy (XPS, Thermo Scientific K-Alpha, USA); Nitrogen adsorption experiments were carried out on an AutosorbiQ analyser (Florida, USA); Thermogravimetric analysis (TGA) was recorded on a thermogravimetric analyser (Zurich, Switzerland); The power for the EE-SPME experiments was provided by a HY3005ET DC regulated power supply (Huayi Electronics, China); A CHI-660C electrochemical workstation (Shanghai Chenhua Co., China) was used for electrochemical measurements. Water was purified with a Milli-QIntegralCabinet3 ultrapure water system (MiliBoCompany, USA).

The GC-FID conditions: An initial temperature of 150 °C (held for 1 min), followed by an increase at 15 °C/min to 250 °C (held for 1 min), and 6 °C/min to 273 °C. The run time was 13 min. The FID temperature was 300 °C.

The GC–MS conditions: The oven temperature was initially set at 80 °C for 1 min, then gradually increased to 250 °C at a rate of 10 °C per min. Subsequently, the temperature was decreased to 8 °C per min until it reached 280 °C, where it was maintained for a duration of 5 min. A shunt injection was conducted with a shunt ratio of 10:1, utilizing helium as the carrier gas at a flow rate of 0.8 mL min^{-1} and an injection volume of 1 μL. The mass spectrometer was operated in electron impact (EI) mode. Pre-column pressure: 70 kPa. Injection temperature: 250 °C. Ion source: EI (200 °C). Interface temperature: 280 °*C. electron* energy: 70 eV. Solvent delay: 5.5 min. For qualitative analyses, full scan mode was used with a scan range of 40–400 *m/z*. For quantitative analyses, selective ion mode was used and m/z 79 was selected as the ion fragment for ALA, EPA, and DHA.

2.3. Fabrication of the HLB-An bonded SSW

The selection of appropriate fiber coating materials plays a crucial role in the process of SPME. HLB can be obtained with suitable hydrophilic (NVP) and lipophilic (DVB) monomers **(**Fig. 1A**)**. Homemade HLB was prepared according to the previous literature with some modifications (Karki et al., 2021). NVP/DVB feed ratios of 30:70 (M/M) was mixed using toluene as a pore forming agent. Take 8.5 mL of distilled water into a 50 mL three-necked flask, add 0.042 g of hydroxypropylmethylcellulose powder, stir well to dissolve, as a dispersed phase standby. Precisely measure 2 mL toluene, 0.35 mL n-dodecane, 0.6 mL N-vinylpyrrolidone and 1.44 mL divinylbenzene to a small beaker, add 0.016 g AIBN, mix well and then poured into a three-necked flask, rapid stirring for 30 min, heated to 70 °C, condensing and refluxing stirring reaction for 12 h after the reaction was stopped, the product was washed with water and methanol for several times, centrifugal separation and then dried under vacuum for 12 h at 80 °C.

Chloromethylated HLB was first prepared by chloromethylation reaction, adding 0.5 g HLB, 1.91 mL (0.022 mol) hydrochloric acid, 0.69 g (0.022 mol) $(CH_2O)_n$, 3.1 g (0.022 mol) $ZnCl_2$ in 50 mL three-necked flask, and the reaction was carried out by reflux reaction for 3 h at 80 °C under N_2 protection. At the end of the reaction, the sample was washed with distilled water to neutral, and then washed with anhydrous ethanol for 2 times, and finally dried in an oven at 80 °C for 12 h to obtain a light-yellow solid (HLB-CH_2Cl). In a 50 mL three-necked flask, 0.5 g of HLB-CH_2Cl, 16 mL of (0.25 mol) acetone, and 0.59 mL of aniline were added and dispersed by sonication for 3 min. Then the reaction was carried out at 70 °C for 12 h under stirring at 100 r min^{-1}. The sample obtained was rinsed with anhydrous ethanol for 5 times and dried in an oven at 80 °C for 18 h. A yellowish solid was obtained, i.e., HLB-An.

While these solid particles exhibit favorable extraction capabilities, their lack of adhesion to the coated substrate necessitates the use of an adhesive to secure them in place (Wu, Liu, Tian, Wu, & Zhao, 2021). The prepared HLB-An was bonded to the stainless-steel wire etched by aqua regia using graphene-epoxy resin as an adhesive, and then the stainless-steel wire was then assembled into the gas phase injection needle **(**Fig. 1B**)**. After bonding, it was oven-cured at 60 °C for 10 min.

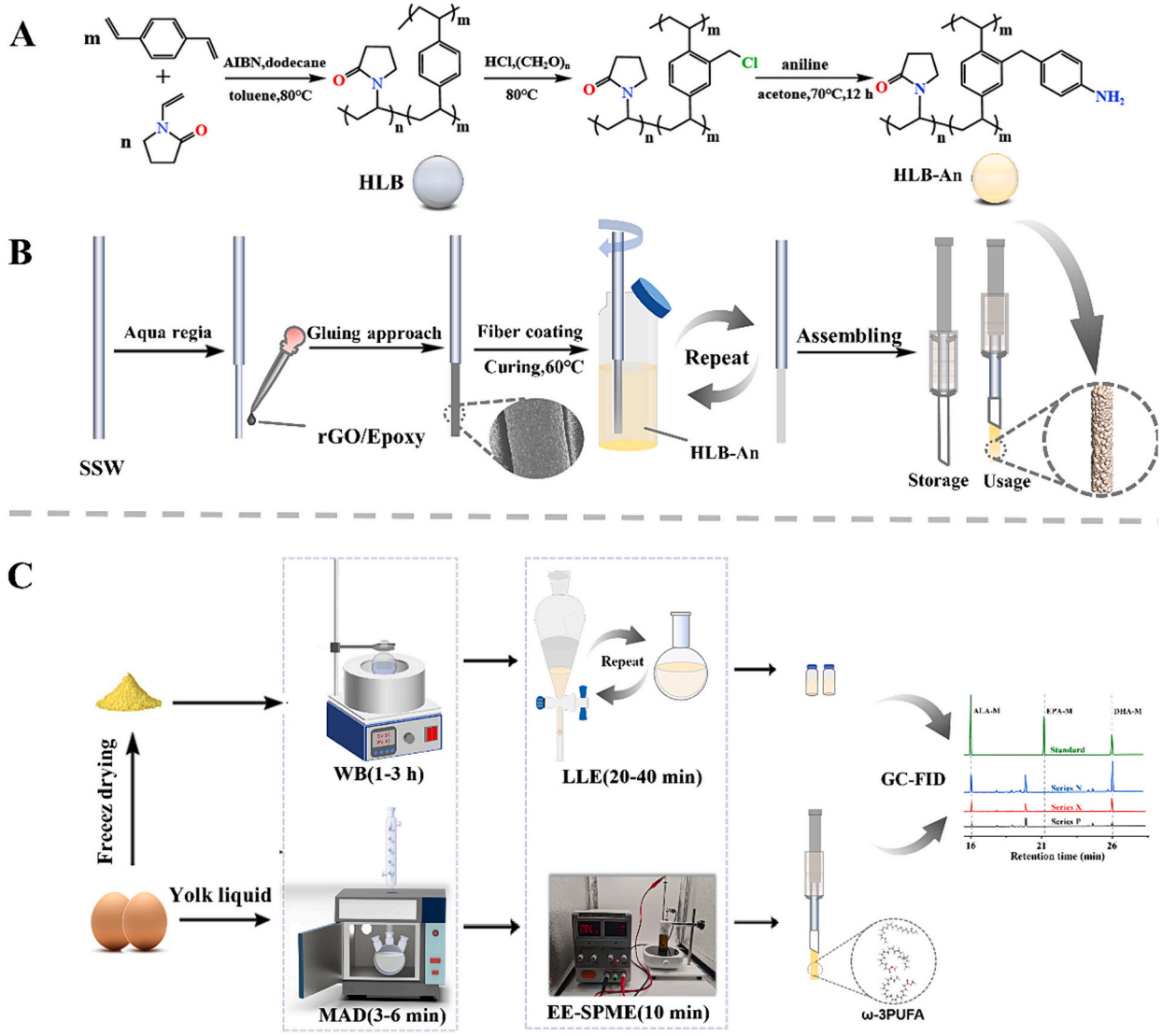

Fig. 1. Schematic diagrams of (A) the synthesis of HLB-An; (B) preparation of SSW-HLB-An; (C) MAE-EE-SPME.

2.4. Eggs samples treatment

Both regular and ω-3 PUFA-enriched eggs were purchased from a local supermarket (Wuxi, China). The yolks and whites of the egg samples were separated, mixed, and stirred well and stored at −20 °C. The yolk liquid was divided into two equal portions, one of which was vacuum freeze-dried in a freeze-dryer for 48 h. Subsequently, its weight was measured, and its moisture content was determined and used for comparison tests. The other portion was weighed directly for the MAE process.

Fatty acid methyl esterification in eggs was required for conversion to the corresponding fatty acid methyl esters. The lyophilized samples were determined by a modified conventional method using sealed BF_3-CH_3OH saponification and esterification, and the results were compared with those obtained from egg yolk liquids assayed by microwave catalysis. Besides, the effect of matrix on ω-3 PUFAs in three different brands of eggs was verified. The matrix effects values (%ME) were calculated using the following eq. 2.1 (Pano-Farias, Ceballos-Magana, Muniz-Valencia, & Gonzalez, 2017):

$$ME\% = \left[1 - \left(\frac{Slope_{solution}}{Slope_{matrix-matched}}\right)\right] \times 100\% \quad (2.1)$$

where $Slope_{solution}$ represents the slope of the solution calibration curve, $Slope_{matrix\text{-}matched}$ represents the slope of the matrix-matched calibration curve.

2.4.1. Experimental procedure for the sealed BF_3-methanol saponification esterification method

The classical sealed BF_3-methanol saponification esterification method was employed according to the literature (Simčič, Stibilj, & Holcman, 2011). A 2.00 g sample of egg yolk powder was placed into a liposuction tube for measurement. Add gallic acid, 1 mL of C11 internal standard solution and 10 mL hydrochloric acid, stir well, put into 80 °C constant temperature water baths to hydrolyze for 30 min, add 10 mL ethanol, stir well. Add 25 mL of anhydrous ether, shake for 1 min. Add 25 mL of petroleum ether, shake for 1 min, transfer the organic layer. The lipid extraction process was repeated 3 times, and the extract was evaporated and concentrated to near dryness. After concentration, add 10 mL of KOH methanol solution, add 70 °C water bath reflux 5–10 min, then add 5 mL of BF_3 methanol solution, continue to reflux for 10 min. 3 mL of saturated sodium chloride solution washed for three times, centrifuged at 5000 r/min for 5 min, and then take the supernatant and determined by GC-FID.

2.4.2. MAE procedure

An accurately weighed 20 mg of egg wash was transferred to a 25 mL flat-bottomed vial and mixed successively with saponification esterification reagents (chloroacetyl methanol solution, BF_3, KOH, etc.), and additives (2,2-dimethoxypropane (DMP)) and sonicated for 10 min. The samples and standard solution were subsequently subjected to esterification under optimized conditions (microwave power, microwave treatment time) (Fig. 1C). The treated mixture was diluted with phosphate buffer solution (PBS) (v:v = 1:99, 0.1 mL: 9.9 mL) and the dilution was used for EE-SPME.

2.5. EE-SPME procedure

The EE-SPME unit consisted of a DC regulated power supply, a platinum wire electrode, a sample cell, and HLB-An adhesive solid-phase microextraction fibers. Briefly, 15 mL of sample or standard solution was placed in a 20 mL glass vial with a stir bar. HLB-An/SSW needed to be aged at 300 °C for 1 h before use. The aged SPME fiber was immersed in standard or sample solutions to extract the target, and platinum wire electrode was immersed in the solutions to form a complete electric field system (Fig. 1C).

During the extraction process, the sample solution was stirred using a magnetic stirrer at a speed range of 0–1400 rpm. After enrichment extraction, the fiber head was pulled back into the injector and immediately introduced into the inlet of the GC for thermal desorption at a desorption temperature of 280 °C.

2.6. Method validation

The developed MAE-EE-SPME-GC-FID method was evaluated by linearity, limit of quantification (LOQs, signal-to-noise ratios (S/N) = 10), limit of detection (LODs, $S/N = 3$), recovery, and relative standard deviation (RSD). Repeatability (6 times per day) and neutrality (3 consecutive days) were tested.

3. Result and discussion

3.1. The design of esterification and extraction for ω-3 PUFAs

Esterification is the process of producing esters from carboxylic acids and alcohols. An ester is formed when the -OH group of a carboxylic acid is replaced by the alkoxy group of an alcohol. Catalyst was required for the esterification process. The catalyst was used to reduce the activation energy barrier of the esterification process. Moreover, heat should be provided as an energy source and no reaction occurs between the carboxylic acid and the alcohol. Microwaves could transfer energy directly to the reactants without preheating and might reduce the activation energy barrier of the reaction (H. Li, Zhang, Pang, Li, & Gao, 2020), thus microwave was used as a heating energy source for the esterification reaction of ω-3 PUFAs.

ω-3 PUFAs are polar molecules with molecular dimensions between 15.83 and 19.68 Å **(Fig. S1, Fig. S2)**. An HLB-An-based extraction fiber (HLB-An/SSW) was used as a working electrode for EE-SPME of ω-3 PUFAs. Specifically, HLB was a polymer with a homogeneous pore size of about 5.77 nm, large specific surface area and hydrophilic and lipophilic properties (Murakami et al., 2018). The aniline-modified HLB enhanced the polarity of HLB possibly facilitating its adsorption of polar ω-3 PUFAs. Furthermore, the electrochemical and thermodynamic properties of HLB-An were also improved. Combined with GC-FID, the MAE-EE-SPME method was used for the determination of ω-3 PUFAs (ALA, EPA, DHA) in three different brands of eggs (N-Series, X-Series, P-Series) (Fig. 1C).

3.2. Characterization of HLB-An/SSW

3.2.1. Structural characterization of HLB-An

The morphology of HLB-An and SSW fibers was characterized using optical microscope (Fig. 2A, Fig. 2C) and SEM (Fig. 2B, Fig. 2D). The surface of smooth SSW became rough after erosion by aqua regia **(Fig. S3A-D)**, and the HLB-An completely covered the SSW. The graphene-epoxy coating covered the fiber surface uniformly and completely **(Fig. S3E-F)**. HLB had an obvious spherical structure with the intact microspheres, which consistent with reported morphology (Karki et al., 2021). HLB-An had a relatively rougher surface compared to HLB, resulting in an increase in the number of adsorption sites of the material, with diameters ranging from 5 μm to 20 μm. Combined with the microscope image, it revealed that the microspheres become slightly yellowish **(Fig. S4A-D)**.

The permanent porosity of HLB and HLB-An was evaluated by N_2 adsorption-desorption isotherm (Fig. 2E, **Fig. S5)**. Calculations from the adsorption data showed that both HLB and HLB-An had large Brunauer-Emmett-Teller surface area (S_{BET}) of 767.93 $m^2\ g^{-1}$ and 828.27 $m^2\ g^{-1}$, and Langmuir surface areas ($S_{Langmuir}$) of 2909.73 $m^2\ g^{-1}$ and 3834.34 $m^2\ g^{-1}$, respectively. The large specific surface areas led to an increase in the adsorption sites of the HLB-An, which improved the detection sensitivity. The average pore sizes of HLB and HLB-An were 5.77 nm and 5.97 nm **(Fig. S5)**, respectively, suggesting that HLB-An was mesoporous. **Fig. S2** illustrated the spatial configurations of ω-3 PUFAs, which showed that with the increase of carbon chains and carbon-carbon double bonds, the structures of the targets were more curled, in which methyl linolenate (ALA-M) had the longest molecular diameter of 19.687 Å, and methyl eicosapentaenoic acid (EPA-M) and methyl docosahexaenoate (DHA-M) reached 16.312 Å and 15.833 Å, respectively. It indicated that the HLB-An could provide sufficiently large nanochannels for the movement and adsorption of the analytes. It demonstrated the existence of a pore-size matching effect between HLB-An and ω-3 PUFAs (J. Li et al., 2023).

The elemental composition and chemical bonding of HLB and HLB-An were investigated using XPS. Characteristic elemental peaks of C 1 s, N 1 s and O 1 s were present in the XPS spectra of both HLB and HLB-An **(Fig. S6A)**. Comparing HLB to HLB-An, the N 1 s atomic percentage increased from 1.72% to 3.94% and a small amount (0.22%) of Cl remained, which corresponded to the chloromethylation of HLB and the incorporation of N in aniline **(Table S1)**. The peaks located at 284.8, 285.6, and 288.6 eV in the C 1 s high-resolution spectrum were ascribed to the C-C, C-O, and C=O characteristic peaks, respectively **(Fig. S6B)**. In high-resolution XPS spectrum of the N 1 s **(Fig. S6C)**, the peaks centered at 399.65 and 401.81 eV, matching with N-H and N–C=O of the amino groups from the HLB-An (Wang et al., 2019). In the case of O 1 s **(Fig. S6D)**, the HLB had a characteristic peak at 532.78 eV corresponding to C=O, and the HLB-An peak at 532.28 eV with a trace offset.

Fig. S7 presented the XRD patterns of HLB and HLB-An. The XRD diffraction peak of HLB was located at 17°, and the diffraction peak corresponding to 17° disappeared for HLB-An after-amination treatment. It showed that the crystalline form of HLB and HLB-An changed more significantly with the structures of the two changed slightly combined with the SEM images. It was hypothesized that the cause of this phenomenon may be the formation of aniline attached to the HLB surface.

The structure information of HLB and HLB-An were characterized by FT-IR spectrum **(Fig. S8)**. The spectrum revealed that a prominent absorption peak at 1685.9 cm^{-1} attributed to the stretching vibration of the C=O group in the NVP (Zhang et al., 2023). In addition, a strong absorption peak at 1600.6 cm^{-1} was observed, corresponding to the backbone vibration of the benzene ring of DVB. Furthermore, the vicinity of the out-of-plane bending vibration of the neighboring hydrogen atoms on the para-disubstituted benzene ring of DVB exhibited a distinct characteristic at 830.1 cm^{-1} (Yao et al., 2019). Lastly, the vicinity of the peak of C=O stretching vibration in the structure of NVP was indicated

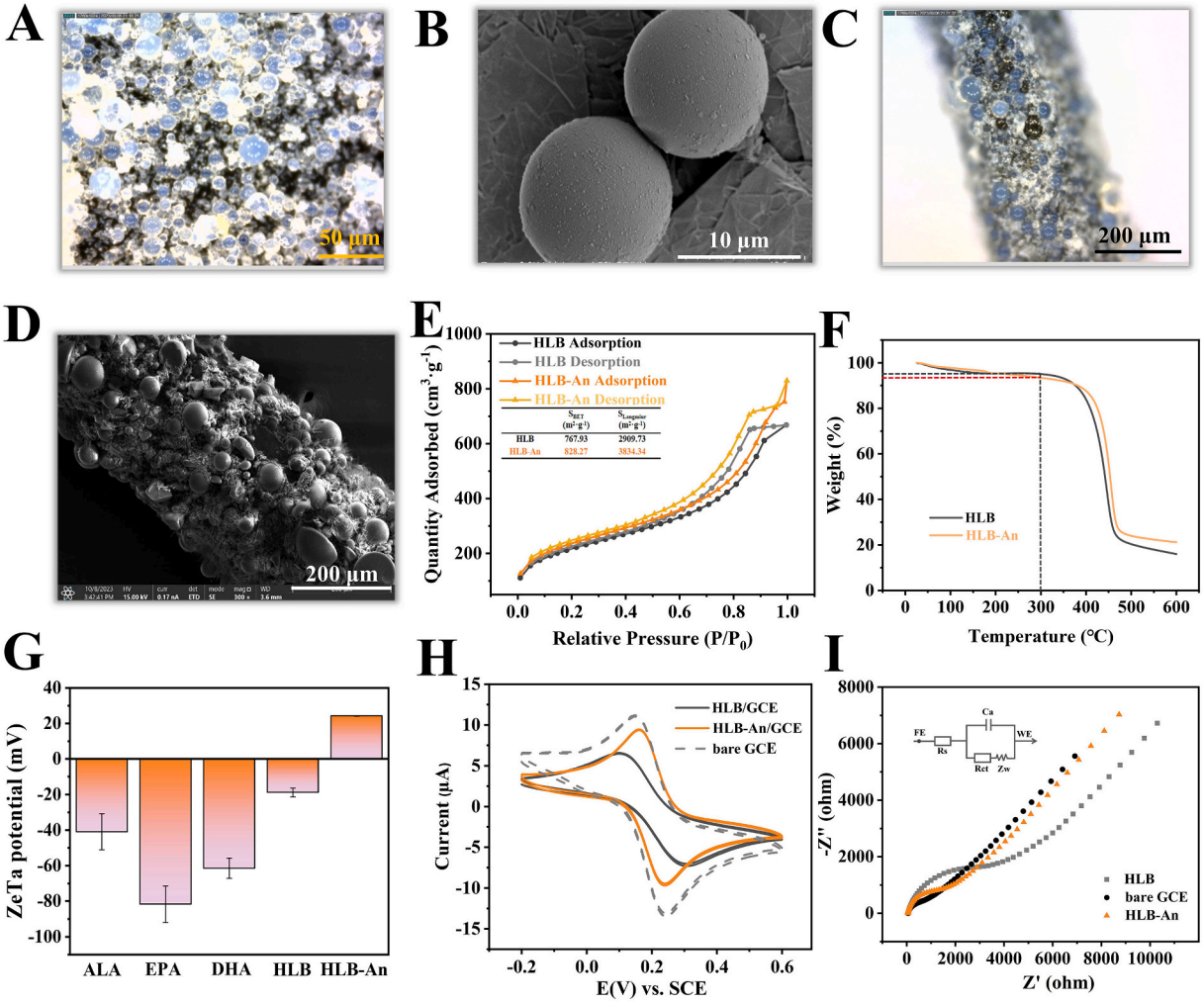

Fig. 2. Microscope images of (A) HLB-An, (C) HLB-An/SSW; SEM images of (B) HLB-An, (D) HLB-An/SSW; (E) N_2 adsorption-desorption isotherms and (F) TGA curves of HLB and HLB-An; (G) ZeTa potentials of ALA, EPA, DHA, HLB, and HLB-An; (H) CV and (I) EIS curves of bare GCE, HLB/GCE and HLB-An/GCE in 1.0 mmol L^{-1} $[Fe(CN)_6]^{3-/4-}$ (+0.2 mol L^{-1} KCl) (CV scan rate: 40 mV s^{-1}).

at 300.2 cm^{-1}, indicating the successful polymerization of NVP and DVB (Liu et al., 2020; Sinha & Purkait, 2014). The strong spectral bands in the ranges of 1400–1650, 3000–3100 and 2800–3000 cm^{-1} were attributed to the stretching vibration of the aromatic ring (C=C), aromatic C-H stretching vibration and the stretching vibration of methylene C-H respectively. In addition, peaks were found at 795.4 and 707.2 cm^{-1}, which may be related to the bending vibration of aromatic C-H. The vibrational absorption of the amino group in aniline gave rise to a notable characteristic peak at approximately 3300 cm^{-1}, indicating the presence of aniline (Meng-Xia & Yuan, 2002).

3.2.2. *Electrochemical and thermal properties of HLB-An/SSW*

SPME coupled with GC was a classical method (Ren et al., 2024). Due to the high temperature of the inlet port (around 300 °C), the thermal stability of the extracted fiber coating was required. Therefore, a comparison of the thermal stability of HLB and HLB-An was made using TGA. There was about 2% weight loss of the HLB-An at 0–200 °C, which might be since some water molecules and organic solvents remain in the pores **(**Fig. 2**F)**. Subsequently up to 350 °C, HLB still had good thermal stability and combined with the derivative thermogravimetry (DTG) plot **(Fig. S9)**, which showed that the thermal stability of the HLB-An was higher than that of HLB, making the coating suitable for GC thermal desorption.

Examining the charged properties of HLB-An and targets, the HLB was negatively charged (ζ = −12.4 mV), and after amine functionalization, the HLB-An material had a positive charge (ζ = 23.0 mV), and the ω-3 PUFAs were all negatively charged to varying degrees (ζ = −40.9, −81.7, and − 61.4 mV), thus suggesting that the HLB-An had a negative charge on the targets with electrostatic force **(**Fig. 2**G)**. Cyclic voltammetry (CV) and electrochemical impedance spectroscopy (EIS) were investigated for HLB and HLB-An modified GCE **(**Fig. 2H-I**)**. The HLB-An exhibited a better electron diffusion and electrostatic attraction than the HLB. On this basis, the CV curves of HLB/GCE and HLB-An/GCE for 1.0 mmol L^{-1} $[Fe(CN)_6]^{3-/4-}$ redox probes were explored at sweep rates of 20–200 mV s^{-1} to compare their chemical performances **(Fig. S10)**. The Randles-sevick eq. 3.1 listed as follows.

$$I_p = 2.69 \times 10^5 A C D^{1/2} n^{2/3} v^{1/2} \quad 3.1$$

where Ip was the response current (A), A was the electrochemically active surface area (cm^2), C was the system concentration of the $[Fe(CN)_6]^{3-/4-}$ redox probe (mol/cm^3), D was the diffusion coefficient of the $[Fe(CN)_6]^{3-/4-}$ (7.60×10^{-6} cm^2 s^{-1}), n was the number of electron transfers for the redox reaction ($n = 1$), and v was the sweeping velocity (V s^{-1}). The electrochemically active areas (Y.-H. Pang, Huang, Wang, Shen, & Wang, 2020), Ipa and Ipc of HLB/GCE and HLB-An/GCE, increased with the increase of sweep speed and were proportional to $v^{1/2}$. The electrochemically active surface areas of HLB/GCE and HLB-An/GCE were calculated to be 1.24 mm^2 and 4.91 mm^2, respectively,

by linear fitting of I_p-$v^{1/2}$, indicating that the HLB-An was more electrochemically active (3.95 times) than HLB.

The charge transfer characteristics of the electrode materials were investigated by EIS (Fig. 2I), which were synchronized with the CV. The resistance of HLB-An was significantly lower compared to HLB. The results indicate that HLB-An could promote the electron transfer process on the electrode surface and had a higher conductivity than HLB.

3.3. MAE procedure

3.3.1. Optimization of MAE

Catalyst type and dosage, microwave irradiation power, microwave irradiation time and DMP dosage were optimized by analyzing 10 mL of the standard solution (800 μg L^{-1}) with GC-FID to obtain the optimal esterification efficiency.

Catalysts can promote the nucleophilic activity of oxygen atoms on carboxyl groups in esterification reactions (Yan, Ma, Deng, & Luo, 2021), and different catalysts catalyze the esterification reactions differently **(Fig. S11)**. The effect of different catalysts (BF_3, acetyl chloride, H_2SO_4, KOH, NaOH, $NaOCH_3$, tetramethylammonium hydroxide (TMAH), and trimethyl sulfur hydroxide (TMSH)) and the amount of addition (2–10 mL) on the efficiency of esterification were compared as shown in Fig. 3A. The results showed that 8 mL of 14% BF_3 were the most effective as catalysts for the esterification of fatty acids in egg yolks. After the preliminary test, the time of saponification treatment and reagent selection had little influence on the results, so The 5 mL KOH methanol solution was selected for 2 min saponification.

Generally, for microwave catalyzed chemical reactions, the higher the microwave irradiation power the higher the yield for the same reaction time (Lieu, Yusup, & Moniruzzaman, 2016). 500–900 W was selected as the heating power **(**Fig. 3B**)**, and the response value of fatty acid methyl ester was higher with the increase of microwave power, and 800 W was selected as the microwave heating power for this experiment in consideration of the safety issues and possible by-products at high power.

In conjunction with the examination of esterification kinetics, the esterification reaction achieved near-completion upon reaching a reaction time of 5 min, which was chosen as the appropriate microwave heating time. The potential safety risk posed by the rapid heating rate associated with microwave heating necessitates the recommendation to cease the heating program after a continuous operation of 2 min, followed by intervals of cooling lasting 1 min to mitigate these hazards.

The esterification reaction was reversible, during the esterification process, the carboxyl group of fatty acid and the hydroxyl group of methanol were dehydrated and condensed to form fatty acid methyl ester, so in addition to the water that may be left in the sample there was also a constant generation of water during the reaction, which affected the efficiency of esterification. Based on the above optimized conditions, DMP was added, which reacts with water to form methanol, and promotes the transesterification reaction while reducing the amount of methanol, which was suitable for water-containing samples, and the effect of different additions of DMP on the transesterification efficiency was investigated in the present work. As shown in Fig. 3C, the esterification efficiency was highest when the addition amount was 7.5% of the moisture content of the sample matrix.

3.3.2. Kinetic analysis of microwave esterification

Comparison of the classical sealed water bath esterification reaction with the optimized MAE reaction yielded the corresponding esterification kinetic parameters. Esterification is a second order reaction. In this study, the amount of alcohol was ensured to be greatly excessive, so that the concentration of alcohol could be considered unchanged in the reaction, and the reaction could be simplified to a first-order reaction, and its kinetic equation was shown in Eq. 3.2.

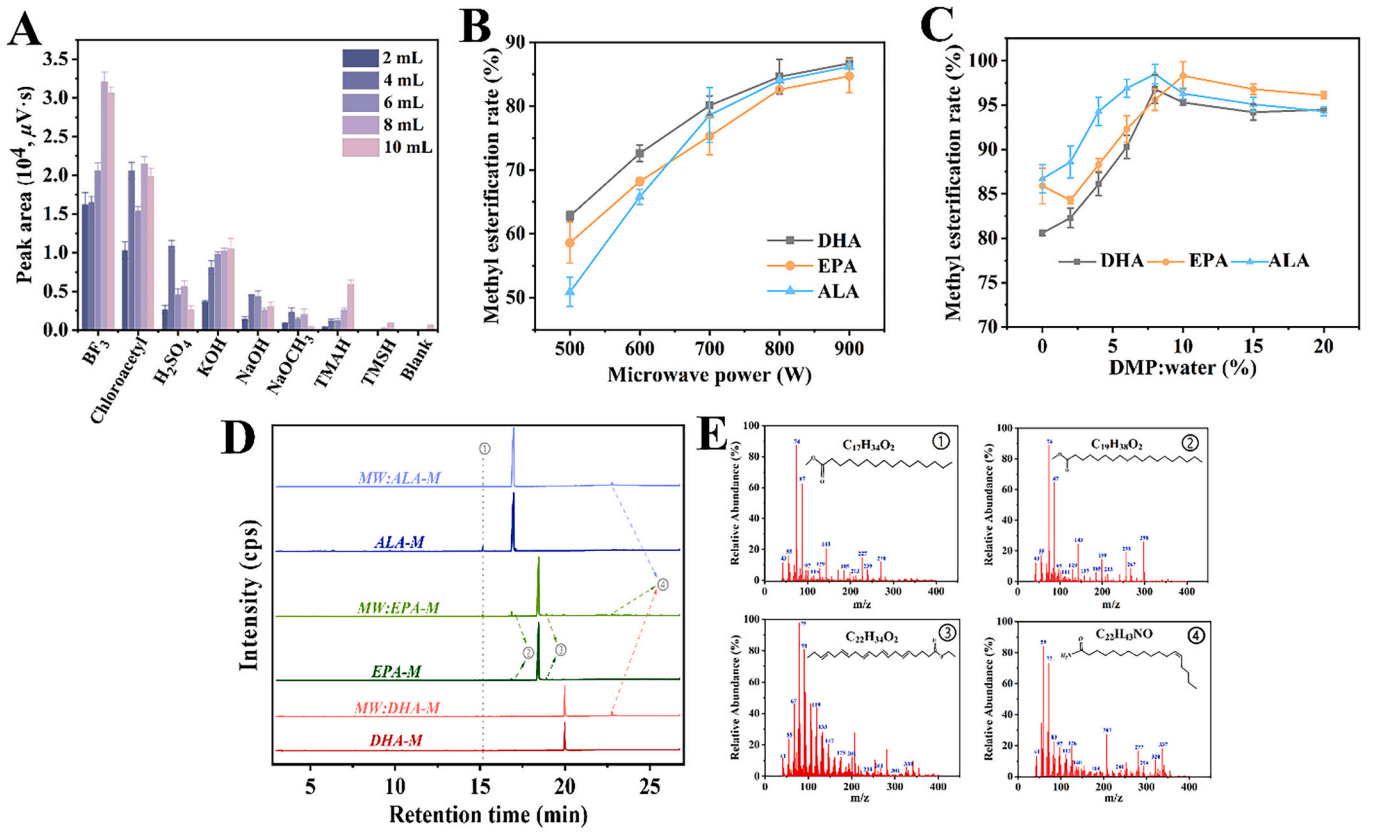

Fig. 3. Effect of the experimental conditions on the esterification efficiency of fatty acid methyl esters (400 μg L^{-1}), including (A) catalyst type and dosage, (B) microwave power and (C) DMP dosage; (D) GC–MS spectra of the three fatty acids before and after the treatment of microwave and (E) product analysis.

$$A + B \rightarrow P$$

$$\frac{-dA}{dt} = \frac{dp}{dt} = k[A][B] = k[A][B0] = k'[A] \quad (3.2)$$

where k' = k[B_0]. As can be seen from the formula, if the concentration of reactant A at different reaction times can be obtained, the reaction velocity constant k 'can be calculated.

The initial concentration (Ce) of ω-3 PUFA standard was set to be 20 mmol L^{-1}, and an excess of methanol was given, the reaction solution was taken at different reaction times and subjected to GC analysis, which

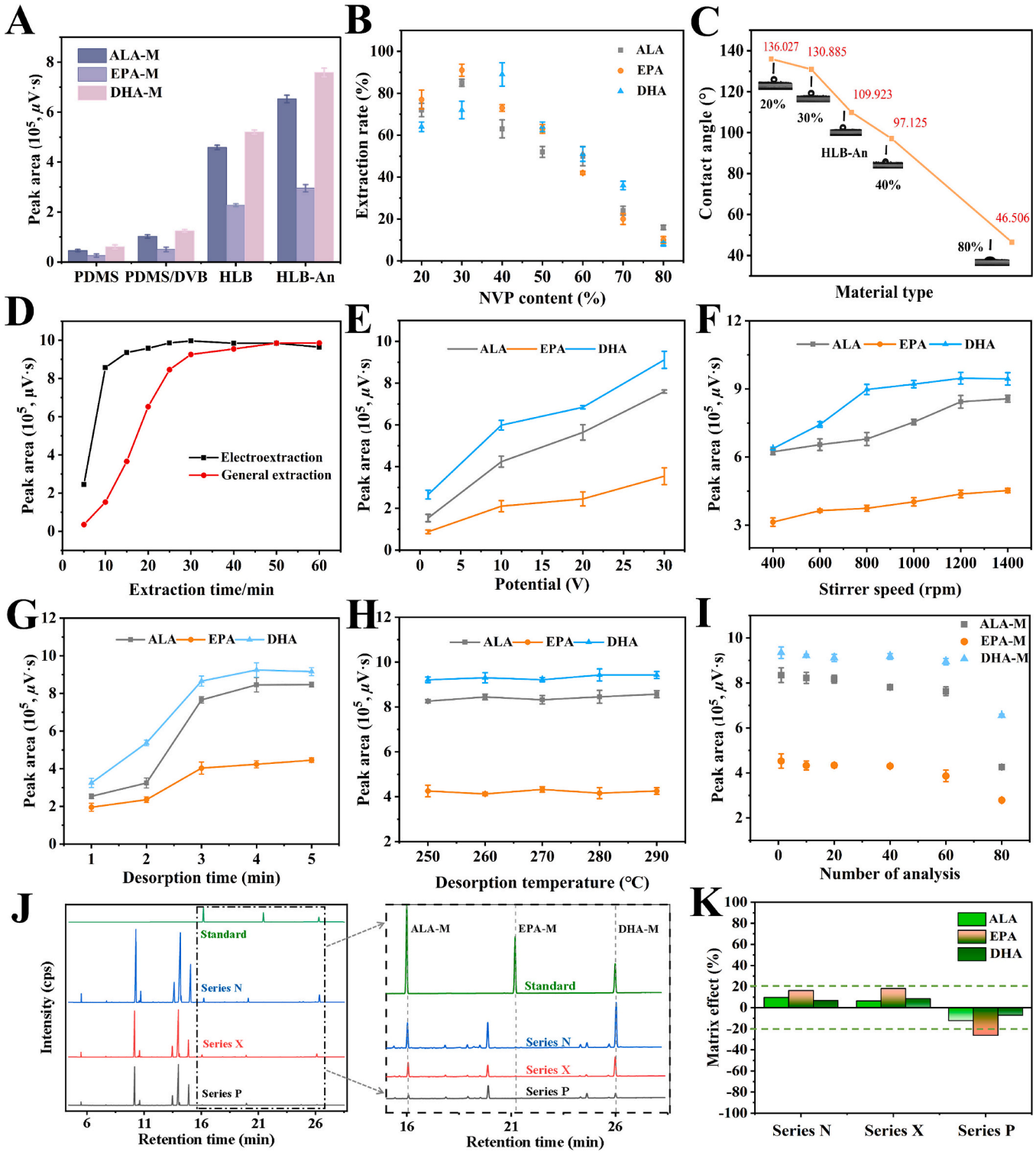

Fig. 4. Comparison of (A) extraction effect of HLB and HLB-An coated material with commercial PDMS and PDMS/DVB; (B) Comparison of adsorption efficiency of HLB with different monomer ratios for fatty acids; Comparison of (C) contact angle of HLB-An synthesized with different ratios of three fatty acids and (D) extraction effect of SPME with HLB-An; Optimizations of conditions for the EE-SPME process for (E) applied potential, (F) stirring speed, (G) desorption time, (H) desorption temperature; (I) stability of SSW/HLB-An (Conditions: eggs spiked with 200 μg L^{-1} fatty acids in working solution; potential 25 V; extraction time, 10 min).; (J) Detection of ω-3 PUFAs in three brands of eggs (series N, series X, series P); (K) Analysis of matrix effects.

can obtain the concentration of aromatic acid Ct corresponding to the time t. On this basis, a linear fit was carried out on t by using ln(Ce-Ct) to obtain the slope of the straight line is -k', and the rate constant could be obtained. A linear regression was performed to obtain the slope of the straight line is -k', which gives the rate constant of the reaction.

The concentration results and kinetic curves for the esterification of each fatty acid and methanol were shown in **Fig. S12** and the kinetic equations were shown in **Table S2**. For the three fatty acids, the classical method took 5.06–10.65 times longer than the microwave-assisted method to achieve close esterification rates.

Although the energy generated by microwaves is non-ionizing radiation, which is much lower than the energy of Brownian motion, and cannot break bonds, it may accelerate the conditions that promote the attainment of certain reactions, which in turn produce by-products. To explore the possible effects of microwave radiation on fatty acids (Kishimoto, 2022), MAE was carried out on ALA-M, EPA-M and DHA-M standards **(Fig. S13A-C)**, respectively. The esterification reagents obtained were analyzed by gas chromatography-mass (GC–MS) spectrometry **(**Fig. 3D-E**)**, which showed that the microwave-catalyzed esterification reaction produced trace amounts of ④ erucic acid amide (< 0.4%), except for the impurities of ① methyl palmitate, ② methyl stearate and ③ ethyl eicosapentaenoate. Microwave-catalyzed esterification reactions were accompanied by the production of by-products, but within an acceptable margin of error.

3.4. Comparison of extraction capacity

While an external electric field was applied to the SPME fiber, targets such as fatty acid methyl esters underwent electromigration, which shortened the extraction time. It can be explained by the partial double bonding nature of the esters due to electron delocalization (Wei et al., 2022). Compared to the two commercial SPME extraction fibers (PDMS and PDMS/DVB) and the HLB fiber coating **(**Fig. 4A**)**, the extraction capacity of HLB-An/SSW for the three fatty acids was 14.30, 11.44, and 12.57 times (ALA-M) higher than that of PDMS, and 6.37, 5.86 and 6.11 times (EPA-M), and 1.42, 1.30 and 1.46 times (DHA-M) of HLB/SSW. The polarity of the coating material played an important role in the significant adsorption of ω-3 PUFAs, and HLB materials can adjust the polarity magnitude by changing the ratio of monomers, which in turn changes the adsorption capacity of polar substances (Karki et al., 2021). As shown in Fig. 4B, by varying the ratio of NVP and DVB (20%–80%), it was found that the adsorption of HLB to the target was better at the ratio of 40%, and therefore the 40% ratio was chosen to synthesize the HLB feedstock for the subsequent experiments. Long-chain fatty acid esters such as PUFA exhibit strong polarity due to the presence of ester groups, and with the growth of the fatty acid carbon chain, PUFA exhibits nonpolar characteristics, whereas the HLB material had hydrophobic crosslinked monomers to form a backbone with a high internal surface area to adsorb the nonpolar compounds, and the NVP as a hydrophilic monomer also enhances the interactions with the polar components. The contact angles of HLB and amine-modified HLB-An at each synthesis ratio were represented in Fig. 4C. As the NVP: DVB increases (20%–80%), the contact angle decreased gradually (136.02°-46.51°), and the contact angle of the amine-modified material (109.92°) was between 30% (130.89°) and 40% (97.13°).

To determine the stability of the fibers, the reusability of the extracted fiber needles were compared in Fig. 4I. There was little change in the extraction efficiency of the extracted fibers after 60 reuses. With further increase in the cycle times, the extraction efficiency decreased, which was probably attributed to the incomplete desorption of ω-3 PUFAs from HLB-An, resulting in the reduction of adsorption sites. Compared with the general SPME method, this extractor needle had good reusability, but still not as good as the extractor needle with membrane protection (>100 times), and the durability of the extractor needle can be further improved by considering the introduction of the membrane protection method in the subsequent research work (Qiao et al., 2022).

3.5. Optimization of EE-SPME procedure

Applied potential, stirring speed, ionic strength, desorption time and temperature were optimized by analyzing 10 mL of the standard solution (800 μg L^{-1}) with an GC-FID detector to obtain the optimal extraction efficiency.

3.5.1. Effect of voltage

Fig. 4E showed the effect of voltage on extraction efficiency, and similar extraction effect was achieved for DHA with EE-SPME for 10–15 min, which is shorter than the adsorption equilibrium time of SPME (50–60 min), indicating that the applied electric field can effectively promote the extraction of ω-3 PUFAs from modified fibers. The influence of electric potential on the adsorption process was studied within the range of 0–30 V. In the presence of an electric field, the electron cloud density of the fatty acid chains decreases, making the fatty acid esters more susceptible to deprotonation and negative charge. Therefore, the application of a positive voltage facilitates the migration of analytes (Wang et al., 2023). The results can be explained that the increase in mass transfer rate was achieved by applying the electrical and electrostatic power provided by the interaction between the optical fiber top coating and the ω-3 PUFAs. A voltage of 30 V was chosen for follow-up extraction to avoid safety issues caused by excessive voltage.

3.5.2. Effect of stirring speed

For the immersion SPME process, a boundary layer exists between the aqueous phase and the fiber coating, and without agitation, diffusion rate of the target analyte within the boundary layer is very slow, thus increasing the time cost. Agitation speeds were examined in the range of 400 to 1400 rpm **(**Fig. 4F**)**. At speeds below 1000 rpm, the peak area of fatty acid methyl esters increased with increasing stirring speed; further increasing the speed to 1200 rpm decreased the rate of peak area increase. Increasing the stirring speed accelerated the diffusion of analytes from the sample solution into the SPME fibers, which facilitated the attainment of adsorption equilibrium. However, too high a speed resulted in the generation of vortices around the SPME fibers, which adversely affected the stability of the SPME. Therefore, 1000 rpm was chosen for further study.

3.5.3. Effect of desorption time and temperature

Appropriate desorption time and temperature at the inlet not only facilitates full desorption of analytes, but also saves time, prolongs fiber life, and avoids incomplete desorption of analytes. The effect of desorption time on extraction efficiency was investigated in the range of 1–5 min **(**Fig. 4G**)**. The extraction efficiency gradually increased up to 3 min, however, further increase in desorption time (5 min) did not result in significant change in extraction efficiency. The complete desorption of analytes from SPME was confirmed. A desorption time of 3.5 min was chosen. It was demonstrated that the coating material was stable up to 350 °C and met the requirements of fiber at 250–290 °C. The increase in desorption temperature at 250–290 °C resulted in a slight increase in extraction peak area. Although higher desorption temperatures give better results for ω-3 PUFAs, the possible heat loss of the fatty acids should also be considered. Taken together, desorption at 280 °C for 3.5 min was the optimal condition.

3.5.4. Effect of ionic strength

An increase in ionic strength (NaCl) decreases the solubility of nonpolar compounds in the aqueous phase, so the effect of ionic strength on the enrichment effect was investigated in the range of 0 to 30% (*w/v*) **(Fig. S14)**. However, as the ionic strength increased, the opposite phenomenon was observed with a sharp decrease in extraction efficiency. It is possible that the addition of salt to the aqueous solution caused an increase in the viscosity of the solution thereby reducing the mass

transfer rate of the PUFA molecules (Wang et al., 2023), and in order to simplify the extraction conditions and to prolong the lifetime of the SPME fibers, no salt was added to the working solution.

3.6. Analytical method validation

The analytical performance of our prepared HLB-An bonded fibers for EE-SPME of BPA was investigated under optimized conditions. The method was validated by linearity, limit of detection, limit of quantification and precision (RSD). The analytical properties under the optimized conditions are summarized in Table 1. The linear range of the method was 7.5–1000 μg L^{-1} (7.5–500 μg L^{-1} for EPA-M) **(Fig. S15)**. The RSDs of the LOD and LOQ were 3.02% ~ 5.17% and 4.25% ~ 7.56% for the daytime and inter-daytime based on the S/N of 3 and 10, respectively. The fiber-to-fiber relative standard deviation was <6.07%, indicating that the prepared fibers had good reproducible production during application. These results made HLB-An/SSW a good performer in the extraction of long-chain unsaturated fatty acid analogs and a potential candidate for sample pretreatment. The combination of HLB-An/SSW with EE-SPME provided an efficient analysis with a 10-min extraction per sample. In addition, the linear range and LOD of our fibers prepared with less coating material were comparable to previously reported methods (Y. H. Pang et al., 2021; Wei et al., 2022). These results indicated that MAE-EE-SPME is suitable for the pre-treatment process of ω-3 PUFAs in eggs.

3.7. Analysis of real samples and matrix effect

The optimized MAE-EE-SPME-GC-FID method was used for the detection of three series of ω-3 PUFAs **(**Fig. 4J**)**. The same concentration of ω-3 PUFAs standard solution was added to the egg yolk esterification solution and determined. The results obtained were broadly similar to those obtained in other studies and on purchase labelling. The spiked recoveries for the two actual egg samples were 85.82% ~ 106.01%, RSD ≤ 7.10% **(**Table 2**)**.

The results showed that the extraction of ω-3 PUFAs by HLB-An/SSW fibers was reduced due to the presence of matrix effects (Kenessov, Koziel, Bakaikina, & Orazbayeva, 2016). For the main reason for the matrix effect, the usage of immersion extraction puts the matrix in contact with the fiber coating, which may lead to contamination and clogging of macromolecules such as proteins. Matrix effects can be positive or negative and can be classified into three categories: strong matrix effects (> 50% and < −50%), moderate matrix effects (20% ~ 50% and − 50% ~ −20%) and slight matrix effects (−20% ~ 20%) (Rutkowska, Łozowicka, & Kaczyński, 2017). The results indicated that the %ME of three brand egg samples were 6.82% ~ 16.36%,6.5% ~ 18.21%, −26.20% ~ −7.20% respectively. It demonstrated that except for EPA in series P, it showed slight matrix effects, confirming the feasibility of MAE-EE-SPME-GC-FID for determining ω-3 PUFAs in eggs.

Table 1
The analytical data of the proposed method.

Fatty Acids	Linear Range (μg L^{-1})	R^2	LOD (μg L^{-1})	LOQ (μg L^{-1})	RSDs (±SD)		
					Single Fiber		Fiber to Fiber
					Intra-day (n = 6)	Inter-day (n = 3)	
ALA-M	7.5–1000	0.9992	1.01	3.39	3.02	5.61	4.64
EPA-M	7.5–500	0.9994	1.46	4.87	3.24	4.25	6.07
DHA-M	7.5–1000	0.9958	1.54	5.15	5.17	7.56	5.12

Table 2
The concentrations (μg L^{-1}), recoveries (%) and RSDs (%, n = 3) of ω-3 PUFAs in three brands of eggs.

Real samples	Spiked concentration (μg L^{-1})	Recovery(RSD, %)		
		ALA	EPA	DHA
Series N	0	11.57 (1.46)	6.28(0.77)	14.95 (3.54)
	20	96.55 (5.92)	102.41 (6.28)	104.32 (1.36)
	50	89.33 (4.23)	94.32 (4.25)	95.72 (1.27)
	100	96.34 (1.56)	102.56 (1.72)	95.37 (2.95)
Series X	0	12.89 (1.50)	6.63(1.45)	16.21 (3.77)
	20	95.85 (1.24)	85.82 (3.61)	106.01 (2.00)
	50	87.02 (7.10)	96.32 (3.96)	94.31 (1.20)
	100	105.26 (2.11)	98.57 (2.79)	96.03 (3.18)
Series P	0	5.78(2.15)	ND	7.22(1.67)
	20	88.13 (7.62)	86.69 (2.13)	102.94 (2.56)
	50	102.30 (5.50)	99.91 (3.27)	95.02 (1.13)
	100	95.65 (6.52)	101.60 (5.86)	92.60 (2.12)

ND: not detect.

3.8. Comparison with other methods

The established method was evaluated in comparison with previous methods for the determination of ω-3 PUFAs **(Table S3)**. The method has the advantages of low dosage of organic reagents, simple and quick operation, and low detection limit for the sensitive determination of ω-3 PUFAs in eggs. HLB-An was used as the adsorbent with high enrichment factor, low preparation cost and mild conditions, and HLB-An/SSW could be reused >60 times. In addition, this method dramatically reduces the use of organic reagents by the introduction of microwave and electric fields, and drastically shortens the pretreatment time.

4. Conclusion

In this study, a method of MAE-EE-SPME was developed to realize fast esterification and effective enrichment of ω-3 PUFAs. Combined with GC-FID, sensitive detection of three fatty acids was achieved in eggs. The microwave significantly shortened the heating time, and the EE-SPME ensured rapid extraction efficiency while avoiding the use of organic solvents. The developed method provided an effective and rapid pre-treatment program for long-chain non-volatile fatty acids and was expected to be applied to process and detect other fatty acids.

CRediT authorship contribution statement

Xian-Chun Gu: Writing – original draft, Software, Resources, Methodology, Investigation, Conceptualization. **Qiu-Fang Zhang:** Visualization, Supervision, Resources, Project administration. **Yue-Hong Pang:** Writing – review & editing, Validation, Supervision, Project administration, Funding acquisition, Conceptualization. **Xiao-Fang Shen:** Writing – review & editing, Visualization, Validation, Supervision, Project administration, Methodology, Funding acquisition, Conceptualization.

Declaration of competing interest

The authors declare that they have no known competing financial interests or personal relationships that could have appeared to influence

the work reported in this paper.

Data availability

Data will be made available on request.

Acknowledgments

This work was supported by the National Key Research and Development Program of China (2022YFF1100803), and the National Natural Science Foundation of China (22276077, 22076067).

Appendix A. Supplementary data

Supplementary data to this article can be found online at https://doi.org/10.1016/j.foodchem.2024.139060.

References

Bakker, N., Hickey, M., Shams, R., Rivera, C. F., Vlahos, J., Cense, H. A., & Houdijk, A. P. (2023). Oral omega-3 PUFA supplementation modulates inflammation in adipose tissue depots in morbidly obese women: A randomized trial. *Nutrition, 111*, Article 112055. https://doi.org/10.1016/j.nut.2023.112055

Balakrishnan, J., Kannan, S., & Govindasamy, A. (2021). Structured form of DHA prevents neurodegenerative disorders: A better insight into the pathophysiology and the mechanism of DHA transport to the brain. *Nutrition Research, 85*, 119–134. https://doi.org/10.1016/j.nutres.2020.12.003

Bonafini, S., Antoniazzi, F., Maffeis, C., Minuz, P., & Fava, C. (2015). Beneficial effects of omega-3 PUFA in children on cardiovascular risk factors during childhood and adolescence. *Prostaglandins & Other Lipid Mediators, 120*, 72–79. https://doi.org/10.1016/j.prostaglandins.2015.03.006

Brunton, N. P., Mason, C., & Collins, M. J. (2015). Rapid microwave assisted preparation of fatty acid methyl esters for the analysis of fatty acid profiles in foods. *Journal of Analytical Chemistry, 70*(10), 1218–1224. https://doi.org/10.1134/s1061934815100044

Duz, M. Z., Saydut, A., & Ozturk, G. (2011). Alkali catalyzed transesterification of safflower seed oil assisted by microwave irradiation. *Fuel Processing Technology, 92*(3), 308–313. https://doi.org/10.1016/j.fuproc.2010.09.020

Grela, E. R., Knaga, S., Winiarska-Mieczan, A., & Zieba, G. (2020). Effects of dietary alfalfa protein concentrate supplementation on performance, egg quality, and fatty acid composition of raw, freeze-dried, and hard-boiled eggs from Polbar laying hens. *Poultry Science, 99*(4), 2256–2265. https://doi.org/10.1016/j.psj.2019.11.030

ISO17059. (2007). *Oilseeds — Extraction of oil and preparation of methyl esters of triglyceride fatty acids for analysis by gas chromatography*.

ISO5509. (2000). *Animal and vegetable fats and oils —Preparation of methyl esters of fatty acids*.

Javed, A., King, A. J., Imran, M., Jeoh, T., & Naseem, S. (2019). Omega-3 supplementation for enhancement of egg functional properties. *Journal of Food Processing and Preservation, 43*(8). https://doi.org/10.1111/jfpp.14052

Karki, I., Li, P., Vik, E. C., Manzewitsch, A., Divirgilio, E., Brewer, W. E., & Shimizu, K. D. (2021). Absorption properties of monolithic poly (divinylbenzene-co-N-vinylpyrrolidone) over a wide range of monomer ratios. *Reactive and Functional Polymers, 163*, Article 104888. https://doi.org/10.1016/j.reactfunctpolym.2021.104888

Kastelein, J. J., Maki, K. C., Susekov, A., Ezhov, M., Nordestgaard, B. G., Machielse, B. N., & Davidson, M. H. (2014). Omega-3 free fatty acids for the treatment of severe hypertriglyceridemia: The EpanoVa for lowering very high triglyceridEs (EVOLVE) trial. *Journal of Clinical Lipidology, 8*(1), 94–106. https://doi.org/10.1016/j.jacl.2013.10.003

Kenessov, B., Koziel, J. A., Bakaikina, N. V., & Orazbayeva, D. (2016). Perspectives and challenges of on-site quantification of organic pollutants in soils using solid-phase microextraction. *TrAC Trends in Analytical Chemistry, 85*, 111–122. https://doi.org/10.1016/j.trac.2016.04.007

Kishimoto, N. (2022). Reducing free acidity and acrolein formation of omega-3-rich oils by blending with extra virgin olive oil during microwave heating. *AIMS Agriculture and Food, 7*(1), 96–105. https://doi.org/10.3934/agrfood.2022006

Li, H., Zhang, C., Pang, C., Li, X., & Gao, X. (2020). The advances in the special microwave effects of the heterogeneous catalytic reactions. *Frontiers in Chemistry, 8*, 355. https://doi.org/10.3389/fchem.2020.00355

Li, J., Yin, Y., Cheng, T., Chen, H., Yang, L., & Wu, H. (2023). Superior pore size for enhancing the competitive adsorption of VOCs under high humid conditions: An experiment and molecular simulation study. *Journal of Environmental Chemical Engineering, 11*(5), Article 111091. https://doi.org/10.1016/j.jece.2023.111091

Lieu, T., Yusup, S., & Moniruzzaman, M. (2016). Kinetic study on microwave-assisted esterification of free fatty acids derived from *Ceiba pentandra* seed oil. *Bioresource Technology, 211*, 248–256. https://doi.org/10.1016/j.biortech.2016.03.105

Liu, Z., Qi, P., Wang, J., Wang, Z., Di, S., Xu, H., & Wang, X. (2020). Development, validation, comparison, and implementation of a highly efficient and effective method using magnetic solid-phase extraction with hydrophilic-lipophilic-balanced materials for LC-MS/MS analysis of pesticides in seawater. *Science of the Total Environment, 708*, Article 135221. https://doi.org/10.1016/j.scitotenv.2019.135221

Marcet, I., Sáez-Orviz, S., Rendueles, M., & Díaz, M. (2022). Egg yolk granules and phosvitin. Recent advances in food technology and applications. *LWT- Food Science and Technology, 153*, Article 112442. https://doi.org/10.1016/j.lwt.2021.112442

Meng-Xia, X., & Yuan, L. (2002). Studies on the hydrogen bonding of aniline's derivatives by FT-IR. *Spectrochimica Acta Part A: Molecular and Biomolecular Spectroscopy, 58*(13), 2817–2826. https://doi.org/10.1016/S1386-1425(02)00072-0

Muhammad Alinafiah, S., Azlan, A., Ismail, A., Rashid, M. A., & N. K.. (2021). Method development and validation for Omega-3 fatty acids (DHA and EPA) in fish using gas chromatography with flame ionization detection (GC-FID). *Molecules, 26*(21). https://doi.org/10.3390/molecules26216592

Murakami, H., Aoyanagi, T., Miki, Y., Tomita, H., Esaka, Y., Inoue, Y., & Teshima, N. (2018). Effects of hydrophilic monomers on sorptive properties of divinylbenzene-based reversed phase sorbents. *Talanta, 185*, 427–432. https://doi.org/10.1016/j.talanta.2018.03.093

de Oliveira Mendes, T., Porto, B. L. S., Almeida, M. R., Fantini, C., & Sena, M. M. (2019). Discrimination between conventional and omega-3 fatty acids enriched eggs by FT-Raman spectroscopy and chemometric tools. *Food Chemistry, 273*, 144–150. https://doi.org/10.1016/j.foodchem.2017.12.084

Pang, Y. H., Huang, Y. Y., Shen, X. F., & Wang, Y. Y. (2021). Electro-enhanced solid-phase microextraction with covalent organic framework modified stainless steel fiber for efficient adsorption of bisphenol A. *Analytica Chimica Acta, 1142*, 99–107. https://doi.org/10.1016/j.aca.2020.10.061

Pang, Y.-H., Huang, Y.-Y., Wang, L., Shen, X.-F., & Wang, Y.-Y. (2020). Determination of bisphenol A and bisphenol S by a covalent organic framework electrochemical sensor. *Environmental Pollution, 263*, Article 114616. https://doi.org/10.1016/j.envpol.2020.114616

Pano-Farias, N. S., Ceballos-Magana, S. G., Muniz-Valencia, R., & Gonzalez, J. (2017). Validation and assessment of matrix effect and uncertainty of a gas chromatography coupled to mass spectrometry method for pesticides in papaya and avocado samples. *Journal of Food and Drug Analysis, 25*(3), 501–509. https://doi.org/10.1016/j.jfda.2016.09.005

Pasupuleti, R. R., Tsai, P. C., Ponnusamy, V. K., & Chen, N. C. (2022). Green sample pre-treatment technique coupled with UHPLC-MS/MS for the rapid biomonitoring of dietary poly-unsaturated (omega) fatty acids to predict health risks. *Chemosphere, 291*(Pt 1), Article 132685. https://doi.org/10.1016/j.chemosphere.2021.132685

Qiao, J. Y., Pang, Y. H., Yan, Z. Y., & Shen, X. F. (2022). Electro-enhanced solid-phase microextraction with membrane protection for enrichment of bisphenols in canned meat. *Journal of Chromatography A, 1685*, Article 463592. https://doi.org/10.1016/j.chroma.2022.463592

Ren, A., Zhang, Y., Bian, Y., Liu, Y. J., Zhang, Y. X., Ren, C. J., & Feng, X. S. (2024). Pyrazines in food samples: Recent update on occurrence, formation, sampling, pretreatment and analysis methods. *Food Chemistry, 430*, Article 137086. https://doi.org/10.1016/j.foodchem.2023.137086

Rutkowska, E., Łozowicka, B., & Kaczyński, P. (2017). Modification of multiresidue QuEChERS protocol to minimize matrix effect and improve recoveries for determination of pesticide residues in dried herbs followed by GC-MS/MS. *Food Analytical Methods, 11*(3), 709–724. https://doi.org/10.1007/s12161-017-1047-3

Simčič, M., Stibilj, V., & Holcman, A. (2011). Fatty acid composition of eggs produced by the Slovenian autochthonous Styrian hen. *Food Chemistry, 125*(3), 873–877. https://doi.org/10.1016/j.foodchem.2010.09.055

Sinha, M. K., & Purkait, M. K. (2014). Preparation and characterization of novel pegylated hydrophilic pH responsive polysulfone ultrafiltration membrane. *Journal of Membrane Science, 464*, 20–32. https://doi.org/10.1016/j.memsci.2014.03.067

Sprynskyy, M., Monedeiro, F., Monedeiro-Milanowski, M., Nowak, Z., Krakowska-Sieprawska, A., Pomastowski, P., Gadzała-Kopciuch, R., & Buszewski, B. (2022). Isolation of omega-3 polyunsaturated fatty acids (eicosapentaenoic acid - EPA and docosahexaenoic acid - DHA) from diatom biomass using different extraction methods. *Algal Research, 62*, Article 102615. https://doi.org/10.1016/j.algal.2021.102615

Wang, J., Zhang, W., Chen, H., Ding, Q., Xu, J., Yu, Q., … Zhang, L. (2023). Piperazine-linked metal covalent organic framework-coated fibers for efficient electro-enhanced solid-phase microextraction of chlorophenols. *Journal of Chromatography. A, 1692*, Article 463847. https://doi.org/10.1016/j.chroma.2023.463847

Wang, Y., Liu, Y., Wang, H., Liu, W., Li, Y., Zhang, J., & Yang, J. (2019). Ultrathin NiCo-MOF nanosheets for high-performance supercapacitor electrodes. *ACS Applied Energy Materials, 2*(3), 2063–2071. https://doi.org/10.1021/acsaem.8b02128

Wei, L., Wang, D., Sun, J., Wang, X., Shen, Y., & Di, H. (2022). Determination of ten long-chain fatty acids in poppy-seed oil using electro-enhanced solid-phase microextraction-GC/MS. *Food Analytical Methods, 15*(9), 2462–2469. https://doi.org/10.1007/s12161-022-02301-7

Wu, D., Liu, F., Tian, T., Wu, J.-F., & Zhao, G.-C. (2021). Copper ferrite nanoparticles as novel coating appropriated to solid-phase microextraction of phthalate esters from aqueous matrices. *Microchemical Journal, 162*, Article 105845. https://doi.org/10.1016/j.microc.2020.105845

Yadav, G., Yadav, N., & Ahmaruzzaman, M. (2023). Microwave-assisted sustainable synthesis of biodiesel on *Oryza sativa* catalyst derived from agricultural waste by esterification reaction. *Chemical Engineering and Processing Process Intensification, 187*, Article 109327. https://doi.org/10.1016/j.cep.2023.109327

Yan, Z., Ma, Z., Deng, J., & Luo, G. (2021). Mechanism and kinetics of epoxide ring-opening with carboxylic acids catalyzed by the corresponding carboxylates. *Chemical Engineering Science, 242*, Article 116746. https://doi.org/10.1016/j.ces.2021.116746

Yao, Z., Jiao, W., Shao, F., Song, H., Zhang, H., Zhou, Q., & Li, A. (2019). Fabrication and characterization of amphiphilic magnetic water purification materials for efficient

PPCPs removal. *Chemical Engineering Journal, 360*, 511–518. https://doi.org/10.1016/j.cej.2018.12.016

Zhang, Z., Zhu, F., Ma, Y., Huo, Z., Zhang, L., Shen, F., & Zhou, Q. (2023). Preparation of amine-modified amphiphilic resins for the extraction of trace pharmaceuticals and personal care products in environmental waters. *Journal of Chromatography A, 1701*, Article 464062. https://doi.org/10.1016/j.chroma.2023.464062

Zheng, J., Kuang, Y., Zhou, S., Gong, X., & Ouyang, G. (2023). Latest improvements and expanding applications of solid-phase microextraction. *Analytical Chemistry, 95*(1), 218–237. https://doi.org/10.1021/acs.analchem.2c03246